

 Open access • Journal Article • DOI:10.1007/S00397-015-0856-9

Padé approximants for large-amplitude oscillatory shear flow — [Source link](#)

A. Jeffrey Giacomin, [Chaimongkol Saengow](#), [Chaimongkol Saengow](#), [Martin Guay](#) ...+1 more authors

Institutions: [Queen's University](#), [King Mongkut's University of Technology North Bangkok](#)

Published on: 31 May 2015 - [Rheologica Acta](#) (Springer Berlin Heidelberg)

Topics: [Shear stress](#), [Shear rate](#), [Power series](#) and [Padé approximant](#)

Related papers:

- [Exact Analytical Solution for Large-Amplitude Oscillatory Shear Flow](#)
- [Large-amplitude oscillatory shear flow from the corotational Maxwell model](#)
- [A review of nonlinear oscillatory shear tests: Analysis and application of large amplitude oscillatory shear \(LAOS\)](#)
- [Nonlinear Viscoelasticity of Polymer Melts](#)
- [Using large-amplitude oscillatory shear](#)

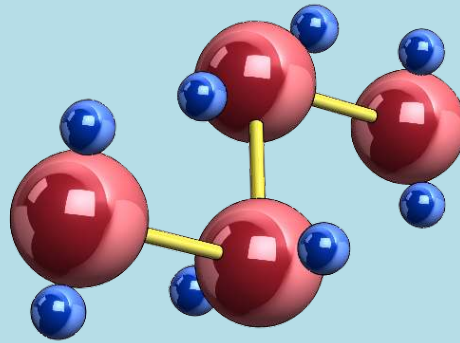
Share this paper:    

View more about this paper here: <https://typeset.io/papers/pade-approximants-for-large-amplitude-oscillatory-shear-flow-5bn37ioa78>

QUEEN'S UNIVERSITY

POLYMERS RESEARCH GROUP

19 Division Street, Kingston, ON, K7L 3N6 Canada



**PADÉ APPROXIMANTS FOR
LARGE-AMPLITUDE OSCILLATORY SHEAR FLOW**

A.J. Giacomin^{1,2,*}, C. Saengow (ชัยมงคล แซ่โจ้ว)^{2,3},
M. Guay¹ and C. Kolutawong (ชาญยุทธ โกลิตะวงษ์)³

¹Chemical Engineering Department

²Polymers Research Group
Queen's University

Kingston, Ontario, CANADA K7L 3N6

³Mechanical and Aerospace Engineering Department
Polymer Research Center

King Mongkut's University of Technology North Bangkok
Bangkok, THAILAND 10800

This report is circulated to persons believed to have an active interest in the subject matter; it is intended to furnish rapid communication and to stimulate comment, including corrections of possible errors.

*Corresponding author (giacomin@queensu.ca)

**PADÉ APPROXIMANTS FOR
LARGE-AMPLITUDE OSCILLATORY SHEAR FLOW**

A.J. Giacomin^{1,2,*}, C. Saengow^{2,3}, M. Guay¹ and C. Kolitawong³

¹Chemical Engineering Department

²Polymers Research Group

Queen's University

Kingston, Ontario, CANADA K7L 3N6

³Mechanical and Aerospace Engineering Department

Polymer Research Center

King Mongkut's University of Technology North Bangkok

Bangkok, THAILAND 10800

ABSTRACT

Analytical solutions for either the shear stress or the normal stress differences in large-amplitude oscillatory shear flow, both for continuum or molecular models, often take the form of the first few terms of a power series in the shear rate amplitude. Here we explore improving the accuracy of these truncated series by replacing them with ratios of polynomials. Specifically, we examine replacing the truncated series solution for the corotational Maxwell model with its Padé approximants for the shear stress response, and for the normal stress differences. We find these Padé approximants to agree closely with the corresponding exact solution, and that, in this way, we learn that in this way, one can nearly eliminate the inaccuracies of the truncated expansions.

* Corresponding author (giacomini@queensu.ca).

CONTENTS

I.	INTRODUCTION	4
II.	ANALYSIS: COROTATIONAL MAXWELL MODEL	7
a.	Shear Stress	7
b.	Normal Stress Differences	11
III.	RESULTS	13
IV.	CONCLUSION	14
V.	ACKNOWLEDGMENT	15
VI.	REFERENCES	31

TABLES

Table I:	Literature on Analytical Solutions for Large-Amplitude Oscillatory Shear Flow	25
Table II:	Dimensional Variables	28
Table III:	Dimensionless Variables and Groups	30

FIGURES

Figure 1:	Orthomorphic isometric sketch of alternating velocity profile in oscillatory shear flow [Eq. (1)]. Cartesian coordinates with origin on the stationary plate. The linear velocity profile results from the assumption that inertial effects can be neglected.....	16
Figure 2.	$[0, 2]$ Padé approximant of Eq. (28) (green) <i>versus</i> Eq. (28) (red) and also <i>versus</i> exact solution [Eq. (21) with Eqs. (22)-(27)] (black) for alternance. Counterclockwise loops of minus dimensionless shear stress, $-S$, <i>versus</i> dimensionless shear rate, $\lambda\dot{\gamma}$, calculated for the 2-constant corotational Maxwell model with $Wi/De = 2$ and $\lambda\omega = 1$	17
Figure 3.	$[0, 4]$ Padé approximant of Eq. (28) (green) <i>versus</i> Eq. (28) (red) and also <i>versus</i> exact solution [Eq. (21) with Eqs. (22)-(27)] (black) for alternance. Counterclockwise loops of minus dimensionless shear stress, $-S$, <i>versus</i> dimensionless shear rate, $\lambda\dot{\gamma}$, calculated for the 2-constant corotational Maxwell model with $Wi/De = 2$ and $\lambda\omega = 1$	18
Figure 4.	$[2, 2]$ Padé approximant of Eq. (28) (green) <i>versus</i> Eq. (28) (red) and also <i>versus</i> exact solution [Eq. (21) with Eqs. (22)-(27)] (black) for alternance. Counterclockwise loops of minus dimensionless shear stress, $-S$, <i>versus</i>	

dimensionless shear rate, $\lambda\dot{\gamma}$, calculated for the 2-constant corotational Maxwell model with $Wi/De = 2$ and $\lambda\omega = 1$	19
Figure 5. $[2, 4]$ Padé approximant of Eq. (28) (green) <i>versus</i> Eq. (28) (red) and also <i>versus</i> exact solution [Eq. (21) with Eqs. (22)-(27)] (black) for alternance. Counterclockwise loops of minus dimensionless shear stress, $-\mathbb{S}$, <i>versus</i> dimensionless shear rate, $\lambda\dot{\gamma}$, calculated for the 2-constant corotational Maxwell model with $Wi/De = 2$ and $\lambda\omega = 1$	20
Figure 6. $[0, 2]$ Padé approximant of Eq. (39) (green) <i>versus</i> Eq. (39) (red) and also <i>versus</i> exact solution [Eq. (21) with Eqs. (22)-(27)] (black) for alternance. Counterclockwise loops of minus dimensionless shear stress, $-\mathbb{S}$, <i>versus</i> dimensionless shear rate, $\lambda\dot{\gamma}$, calculated for the 2-constant corotational Maxwell model with $Wi/De = 2$ and $\lambda\omega = 1$	21
Figure 7. $[0, 4]$ Padé approximant of Eq. (39) (green) <i>versus</i> Eq. (39) (red) and also <i>versus</i> exact solution [Eq. (21) with Eqs. (22)-(27)] (black) for alternance. Counterclockwise loops of minus dimensionless shear stress, $-\mathbb{S}$, <i>versus</i> dimensionless shear rate, $\lambda\dot{\gamma}$, calculated for the 2-constant corotational Maxwell model with $Wi/De = 2$ and $\lambda\omega = 1$	22
Figure 8. $[1, 2]$ Padé approximant of Eq. (42) (green) <i>versus</i> Eq. (42) (red) and also <i>versus</i> exact solution [Eq. (41) with Eqs. (22)-(27)] (black) for alternance <i>versus</i> $[x, y]$. Minus dimensionless first normal stress differences, $-\mathbb{N}_1 = 2\mathbb{N}_2$, <i>versus</i> dimensionless shear rate, $\lambda\dot{\gamma}$, left-clockwise loops calculated for the 2-constant corotational Maxwell model with $Wi/De = 2$ and $\lambda\omega = 1$	23
Figure 9. $[1, 4]$ Padé approximant of Eq. (42) (green) <i>versus</i> Eq. (42) (red) and also <i>versus</i> exact solution [Eq. (41) with Eqs. (22)-(27)] (black) for alternance <i>versus</i> $[x, y]$. Minus dimensionless first normal stress differences, $-\mathbb{N}_1 = 2\mathbb{N}_2$, <i>versus</i> dimensionless shear rate, $\lambda\dot{\gamma}$, left-clockwise loops calculated for the 2-constant corotational Maxwell model with $Wi/De = 2$ and $\lambda\omega = 1$	24

I. INTRODUCTION

In certain circumstances, functions can be usefully approximated with ratios of polynomials, and we attribute the method for getting this set of polynomial ratios to Padé ([1]; see Chapter 1 of [2]). Elements of this set are not equally useful, and indeed, some or even all elements will sometimes be of little use. We call each ratio the $[x, y]$ *Padé approximant*, where x is the order of the numerator, and y , of the denominator. Curiously, when the starting function is itself a truncated series, one or more of the Padé approximants may represent the full series more accurately than the starting function (and sometimes, much more accurately), and rheologists sometimes exploit this useful property [3].

Since its conception in 1935 [4,5,6] oscillatory shear flow has become by far the most popular laboratory method for exploring the physics of polymeric liquids. We generate oscillatory shear flow by confining the fluid to a simple shear apparatus, and then subject one solid-liquid boundary to a coplanar sinusoidal displacement, and thus, the fluid to the following velocity profile (see the coordinate system defined and the flow field illustrated in Figure 1):

$$v_x = \dot{\gamma}^0 y \cos \omega t; v_y = v_z = 0 \quad (1)$$

and hence, to a corresponding cosinusoidal shear rate:

$$\dot{\gamma}_{yx}(t) = \dot{\gamma}^0 \cos \omega t \quad (2)$$

where, in this paper, symbols are defined in Table II and Table III (which follow Tables 2 and 3 of [7]). Using the characteristic relaxation time of the viscoelastic fluid, λ , we can nondimensionalize Eq. (2):

$$\begin{aligned} \lambda \dot{\gamma}_{yx}(t) &= \lambda \dot{\gamma}^0 \cos \lambda \omega (t / \lambda) \\ &\equiv \text{Wi} \cos \text{De} (t / \lambda) \end{aligned} \quad (3)$$

where the Deborah number is given by:

$$\text{De} \equiv \lambda \omega \quad (4)$$

and, the Weissenberg number, by:

$$\text{Wi} \equiv \lambda \dot{\gamma}^0 \quad (5)$$

The dimensionless Eq. (3) suggests that dimensionless solutions to large-amplitude oscillatory shear flow problems shall be written in terms of Wi or De only, and we follow this throughout this work.

Increasing either the Weissenberg number or the Deborah number in Eq. (3) causes the fluid response to depart from Newtonian behavior. We can construct a complex dimensionless number from the ordered pair (De, Wi) thus (see this illustrated in Fig. 1 of [7]):

$$\text{Gn} \equiv \text{De} + i \text{Wi} \quad (6)$$

which defines a vector with magnitude:

$$|\text{Gn}| \equiv \sqrt{\text{De}^2 + \text{Wi}^2} \quad (7)$$

and with angle:

$$\phi \equiv \arctan \frac{\text{Wi}}{\text{De}}. \quad (8)$$

The magnitude of G_n reflects how far the fluid behavior departs from Newtonian behavior. We call such departures *non-Newtonian*. We can associate behavior in steady shear flow with $De = 0$, where $G_n = iWi$. We further associate *linear viscoelastic* behavior with $Wi = 0$, where $G_n \equiv De$. The angle ϕ thus reflects the type of departure from Newtonian behavior. The value $\phi = 0$ corresponds to linear viscoelastic behavior, and $\phi = \pi/2$, to steady shear flow.

When higher harmonics are observed in the shear stress response, we call the oscillatory experiment *large-amplitude*. For polymeric liquids, these higher harmonics are commonly observed when:

$$\frac{Wi}{De} > 1 \quad (9)$$

which is when the shear stress and the normal stress difference responses generally exhibit higher harmonics. This condition also happens to describe when the measurements become especially challenging [8,9,10,11]. Eq. (9) is thus our working definition of large-amplitude oscillatory shear flow [12,13], and with recent advances in rheometry, conducting experiments satisfying Eq. (9) is now commonplace for exploring the physics of polymeric liquids [14]. The material functions in this flow are most commonly defined as coefficients of the Fourier series:

$$\frac{\tau_{yx}(\tau, \gamma_0)}{\gamma_0} \equiv - \sum_{\substack{n=1 \\ \text{odd}}}^{\infty} G'_n(\omega, \gamma_0) \sin n\tau + G''_n(\omega, \gamma_0) \cos n\tau \quad (10)$$

where $\tau = \omega t$. We call this set of coefficients, $G'_n(\omega, \gamma_0)$ and $G''_n(\omega, \gamma_0)$, the *Fourier moduli*. These Fourier moduli are readily obtained from a measured time series $\tau_{yx}(\tau, \gamma_0)$ using the discrete Fourier transform [13]. The notation corresponding to Eq. (10), for the first normal stress difference coefficient, is given in Eq. (179) of [7].

The Fourier moduli in (10) are occasionally expanded in odd powers of γ_0 defining a matrix of frequency dependent nonlinear moduli [15,16,17]:

$$\frac{\tau_{yx}(\tau)}{\gamma_0} = - \sum_{\substack{m=1 \\ \text{odd}}}^{\infty} \sum_{\substack{n=1 \\ \text{odd}}}^m \gamma_0^{m-1} [G'_{mn}(\omega) \sin n\tau + G''_{mn}(\omega) \cos n\tau] \quad (11)$$

where $\tau = \omega t$.

The shear stress response in LAOS has also been expanded in odd powers of $\dot{\gamma}^0$, defining a matrix of frequency dependent nonlinear viscosities [18]:

$$\frac{\tau_{yx}(\tau)}{\dot{\gamma}_0} = - \sum_{\substack{n=1 \\ \text{odd}}}^{\infty} \sum_{\substack{m=1 \\ \text{odd}}}^n \dot{\gamma}_0^{n-1} [\eta'_{mn}(\omega) \cos m\tau + \eta''_{mn}(\omega) \sin m\tau] \quad (12)$$

where $(\eta'_{mn}, \eta''_{mn})$ are named the *loss and storage viscosities of mth order*, where $(\eta'_{11}, \eta''_{11}) \equiv (\eta', \eta'')$. The “ m ” in the “ m th order” corresponds to the number of the harmonic in the shear stress response. The “ n ” in the “ m th order” corresponds

to *one plus* the power of the expansion in Eq. (12). The notation corresponding to Eq. (12), for the first normal stress difference coefficient, is given in Eq. (183) of [7]. Finally, the first normal stress difference response in LAOS has been expanded in odd powers of $\dot{\gamma}^0$, defining a matrix of frequency dependent nonlinear coefficients:

$$\Psi_1(\tau) = - \left[\sum_{\substack{p=1 \\ \text{odd}}}^{\infty} \sum_{\substack{m=0 \\ \text{even}}}^{p+1} \dot{\gamma}^0{}^{p-1} \left[\Psi'_{1,m,p+2}(\omega) \cos m\tau + \Psi''_{1,m,p+2}(\omega) \sin m\tau \right] \right] \quad (13)$$

Table I classifies solutions to constitutive equations in large-amplitude oscillatory shear flow for the shear stress that take the form of the truncated power series (Eq. (157) of [7]):

$$\mathbb{S}(\tau) = -A + B Wi^2 - C Wi^4 + \dots \quad (14)$$

or of Eq. (14) further truncated:

$$\mathbb{S}(\tau) = -A + B Wi^2 - \dots \quad (15)$$

where each coefficient A, B, C, \dots is a Fourier series involving odd-valued harmonics. Whereas work on continuum theory employs Eq. (14) (which matches the form of Eq. (28) which is Eq. (58) of [7]), for molecular theory, where calculations are more laborious, Eq. (15) is used (see Eq. (82) of [19]). In this paper, we will compare Eq. (28) with its truncation, Eq. (39), which has the form of Eq. (15). The former comparison will allow us to assess the usefulness of Padé approximants to power series expansions of the form of Eq. (15).

Table I also lists solutions to constitutive equations in large-amplitude oscillatory shear flow for the normal stress differences that take the form of the power series (Eq. (184) of [7]):

$$\mathbb{N}_1(\tau) = -\alpha Wi + \beta Wi^3 - \dots \quad (16)$$

where each coefficient α, β, \dots is a Fourier series involving even-valued harmonics. Below we will replace, Eqs. (14), (15) and (16) each with ratios of polynomials whose power series match Eqs. (14), (15) and (16). These ratios are called Padé approximants. To be clear, the Padé approximant is an approximation of the full series from which the first few terms were used as the starting function.

In this paper, we thus explore the usefulness of Padé approximants for the alternant part of the shear stress and normal stress difference responses to the large-amplitude oscillatory shear flow of polymeric liquids. Specifically, we seek to calculate the Padé approximants to truncated expansions for the alternant parts of the shear stress and normal stress differences responses for a corotational Maxwell fluid. The corotational Maxwell model is the simplest model of fluid viscoelasticity that is relevant to large-amplitude oscillatory shear flow, involving just two parameters: η_0 and λ . By *relevant* we mean that the model predicts, as it should, higher harmonics in the alternant parts of the shear stress and the normal stress differences. We select the corotational Maxwell model because it is not only the simplest relevant model, but also, it is the only relevant constitutive model to have yielded an exact solution for the shear stress in large-amplitude oscillatory shear flow [66].

II. ANALYSIS: COROTATIONAL MAXWELL MODEL

For a single-relaxation time, the corotational Maxwell model is:

$$\mathbb{S} + \lambda \frac{\mathcal{D}\mathbb{S}}{\mathcal{D}t} = -\eta \mathbb{D} \quad (17)$$

in which:

$$\frac{\mathcal{D}\mathbb{S}}{\mathcal{D}t} \equiv \frac{D\mathbb{S}}{Dt} + \frac{1}{2} [\mathbb{W}\mathbb{S} - \mathbb{S}\mathbb{W}] \quad (18)$$

defines the Jaumann derivative; here $D\mathbb{S}/Dt$ is the substantial derivative and:

$$\mathbb{D} \equiv \nabla \mathbf{v} + (\nabla \mathbf{v})^\dagger \quad (19)$$

is the rate-of-strain tensor, and:

$$\mathbb{W} \equiv \nabla \mathbf{v} - (\nabla \mathbf{v})^\dagger \quad (20)$$

is the vorticity tensor. We call the derivative given by Eq. (18) *corotational* because it measures rates of changes of the extra stress tensor with respect to a coordinate frame that both translates and rotates with the fluid. For an extensive discussion of corotational models and their applications, see Chapters 7 and 8 of [20], and also [21,22,23,24,25]. The corotational model framework has been closely connected with molecular theory [26,27,28]. For the limiting behaviours of the corotational Maxwell model in steady shear flow, or in the limit of linear viscoelasticity, see Eq. (50), or Eqs. (37) and (47) below.

a. Shear Stress

Here we assess the usefulness of Padé approximants for improving the accuracy of the truncated expansion for the shear stress response of the corotational Maxwell model in large-amplitude oscillatory shear flow whose exact solution is given by [66]:

$$\mathbb{S}(\tau) = -\frac{1}{De} e^{-\tau/De} \sin\left(\frac{Wi}{De} \sin \tau\right) I_1 - \frac{1}{De} e^{-\tau/De} \cos\left(\frac{Wi}{De} \sin \tau\right) I_2 \quad (21)$$

where:

$$I_1 = De e^{\tau/De} \sum_{k=1}^{\infty} \left[\alpha_k^{(1)} \cos 2k\tau + \beta_k^{(1)} \sin 2k\tau \right] \quad (22)$$

and:

$$I_2 = De e^{\tau/De} \alpha_1^{(2)} \cos \tau + De e^{\tau/De} \beta_1^{(2)} \sin \tau + De e^{\tau/De} \sum_{k=2}^{\infty} \left[\alpha_k^{(2)} \cos(2k-1)\tau + \beta_k^{(2)} \sin(2k-1)\tau \right] \quad (23)$$

and:

$$\alpha_k^{(1)} \equiv \begin{cases} 0 & ;k=0 \\ \frac{-8k^2 \text{De}^2 J_{2k}}{\text{Wi}(4\text{De}^2 k^2 + 1)} & ;k \geq 1 \end{cases} \quad (24)$$

and:

$$\beta_k^{(1)} \equiv \begin{cases} 0 & ;k=0 \\ \frac{4k \text{De} J_{2k}}{\text{Wi}(4\text{De}^2 k^2 + 1)} & ;k \geq 1 \end{cases} \quad (25)$$

and where:

$$\alpha_k^{(2)} = \begin{cases} 0 & ;k=0 \\ \frac{J_{2k} + J_{2k-2}}{\text{De}^2 (2k-1)^2 + 1} & ;k \geq 1 \end{cases} \quad (26)$$

and:

$$\beta_k^{(2)} = \begin{cases} 0 & ;k=0 \\ \frac{\text{De}(2k-1)(J_{2k} + J_{2k-2})}{\text{De}^2 (2k-1)^2 + 1} & ;k \geq 1 \end{cases} \quad (27)$$

By comparing with this exact solution, we can assess how much improvement one might expect from the use of Padé approximants for the shear stress in large-amplitude oscillatory shear flow.

For the corotational Maxwell model, the approximate solution for the dimensionless shear stress response is given by (Eq. (58) of [7]):

$$\begin{aligned}
\mathbb{S}(\tau) = & -\frac{\cos\tau + De\sin\tau}{1+De^2} \\
& + \frac{Wi^2}{4} \left[\frac{3\cos\tau + 6De\sin\tau}{(1+De^2)(1+4De^2)} \right. \\
& \left. + \frac{(1-11De^2)\cos 3\tau + 6(1-De^2)De\sin 3\tau}{(1+De^2)(1+4De^2)(1+9De^2)} \right] \\
& - \frac{Wi^4}{8} \left[\frac{5\cos\tau + 15De\sin\tau}{(1+De^2)(1+4De^2)(1+9De^2)} \right. \\
& + \frac{(5-130De^2)\cos 3\tau + (45-120De^2)De\sin 3\tau}{2(1+De^2)(1+4De^2)(1+9De^2)(1+16De^2)} \\
& \left. + \frac{(1-85De^2+274De^4)\cos 5\tau + (15-225De^2+120De^4)De\sin 5\tau}{2(1+De^2)(1+4De^2)(1+9De^2)(1+16De^2)(1+25De^2)} \right] \\
& + \dots
\end{aligned} \tag{28}$$

which has the form of Eq. (14) where, for the corotational Maxwell model:

$$A \equiv \frac{\cos\tau + De\sin\tau}{1+De^2} \tag{29}$$

and:

$$B \equiv \frac{1}{4} \left[\frac{3\cos\tau + 6De\sin\tau}{(1+De^2)(1+4De^2)} \right. \\ \left. + \frac{(1-11De^2)\cos 3\tau + 6(1-De^2)De\sin 3\tau}{(1+De^2)(1+4De^2)(1+9De^2)} \right] \tag{30}$$

and:

$$C \equiv \frac{1}{8} \left[\frac{5\cos\tau + 15De\sin\tau}{(1+De^2)(1+4De^2)(1+9De^2)} \right. \\ + \frac{(5-130De^2)\cos 3\tau + (45-120De^2)De\sin 3\tau}{2(1+De^2)(1+4De^2)(1+9De^2)(1+16De^2)} \\ \left. + \frac{(1-85De^2+274De^4)\cos 5\tau + (15-225De^2+120De^4)De\sin 5\tau}{2(1+De^2)(1+4De^2)(1+9De^2)(1+16De^2)(1+25De^2)} \right] \tag{31}$$

We examine all Padé approximants of Eq. (14) up to order $[4, 4]$ and, in this corner of the Padé table (see Chapters 1 and 2 of [2]), we find exactly four Padé

approximants, that we next list in order of degree, first of their numerators, then, denominators. Approximant of order $[0, 2]$ of Eq. (14) is given by:

$$\mathbb{S}(\tau) = \frac{-A^2}{A + B Wi^2} \quad (32)$$

of order $[0, 4]$, by:

$$\mathbb{S}(\tau) = \frac{-A^3}{A^2 + AB Wi^2 - (AC - B^2) Wi^4} \quad (33)$$

of order $[2, 2]$, by:

$$\mathbb{S}(\tau) = \frac{-AB + (B^2 - AC) Wi^2}{B + C Wi^2} \quad (34)$$

and finally, of order $[2, 4]$, by:

$$\mathbb{S}(\tau) = \frac{A^2 C - AB^2 - (2ABC - B^3) Wi^2}{AC - B^2 - BC Wi^2 - C^2 Wi^4} \quad (35)$$

Eq. (35) is the first main result of this work. We can also report that this $[2, 4]$ approximant exhibits the correct limiting behaviors, for both steady shear flow:

$$\lim_{De \rightarrow 0} \mathbb{S}(\tau) = \lim_{De \rightarrow 0} \frac{A^2 C - AB^2 - (2ABC - B^3) Wi^2}{AC - B^2 - BC Wi^2 - C^2 Wi^4} = -\frac{1}{1 + Wi^2} \quad (36)$$

which matches Eq. (84) of [7] (see Eq. (50) below) as it should. For linear viscoelasticity:

$$\lim_{Wi \rightarrow 0} \mathbb{S}(\tau) = \lim_{Wi \rightarrow 0} \frac{A^2 C - AB^2 - (2ABC - B^3) Wi^2}{AC - B^2 - BC Wi^2 - C^2 Wi^4} = -\frac{\cos \tau + De \sin \tau}{1 + De^2} \quad (37)$$

which matches Eq (59) of [7] as it should. It goes without saying that all Padé approximants will be singular where their denominators go to zero, and one must, of course, be mindful of this when we use these. The singularities in Eq. (35) arise, for example, whenever the roots of:

$$AC - B^2 - BC Wi^2 - C^2 Wi^4 = 0 \quad (38)$$

are both real and positive.

In Section III below, we will compare the Padé approximants, Eqs. (32) through (35), with the approximate solution from which these were derived, Eq. (28), and then with the exact solution [Eq. (21) with Eqs. (22)-(27)]. For Padé approximants of Eq. (28), we have limited ourselves to the $[4, 4]$ corner of the Padé table, however, were our results unsatisfactory, in any way, we can report that, from experience, extending our search area to a larger corner of the Padé table does not help. By *unsatisfactory*, we at least mean, when the shear stress loops lack two-fold symmetry. In our subsequent treatment of Eq. (39), we get less satisfactory results. Given the usefulness of our $[2, 4]$ approximant, we see no reason to pursue orders exceeding $[4, 4]$.

Mindful of the discussion following Eq. (15) above, we next truncate Eq. (28) to its next lowest power of Wi :

$$\mathbb{S}(\tau) = -\frac{\cos \tau + De \sin \tau}{1 + De^2} + \frac{Wi^2}{4} \left[\frac{3 \cos \tau + 6De \sin \tau}{(1 + De^2)(1 + 4De^2)} + \frac{(1 - 11De^2) \cos 3\tau + 6(1 - De^2)De \sin 3\tau}{(1 + De^2)(1 + 4De^2)(1 + 9De^2)} \right] \quad (39)$$

+...

which has the general form of Eq. (15). We examine all Padé approximants of Eq. (15), up to order $[4,4]$ and we find exactly two Padé approximants, which we next list in order of degree, first of their numerators, then, denominators. Approximant $[0,2]$ matches Eq. (32), and approximant $[0,4]$ is given by:

$$\mathbb{S}(\tau) = \frac{-A^3}{A^2 + ABWi^2 + B^2Wi^4} \quad (40)$$

which is just Eq. (33) evaluated for $C = 0$. We will examine Eqs. (39) and (40) in Section III below.

b. Normal Stress Differences

Here we assess the usefulness of Padé approximants for improving the accuracy of the truncated expansion for the normal stress difference responses of the corotational Maxwell model in large-amplitude oscillatory shear flow. We select the corotational Maxwell model because it is not only the simplest relevant model, but also, it is the only relevant constitutive model to have yielded an exact solution for the normal stress differences in large-amplitude oscillatory shear flow. This exact solution is given by:

$$\mathbb{N}_1(\tau) = -2\mathbb{N}_2(\tau) = \frac{2}{De} e^{-\tau/De} \cos\left(\frac{Wi}{De} \sin \tau\right) I_1 - \frac{2}{De} e^{-\tau/De} \sin\left(\frac{Wi}{De} \sin \tau\right) I_2 \quad (41)$$

where I_1 and I_2 are given by Eqs. (22) and (23). By comparing with this exact solution, we can assess exactly how much improvement one might generally expect from the use of Padé approximants for the normal stress differences in large-amplitude oscillatory shear flow.

For the corotational Maxwell model, the dimensionless normal stress differences are given by (Eq. (66) of [7]):

$$\begin{aligned}
\mathbb{N}_1(\tau) &= -2\mathbb{N}_2(\tau) \\
&= -\text{We} \left[\frac{1}{1+\text{De}^2} + \frac{(1-2\text{De}^2)\cos 2\tau + 3\text{De}\sin 2\tau}{(1+\text{De}^2)(1+4\text{De}^2)} \right] \\
&\quad + \frac{\text{We}^3}{4} \left[\frac{3}{(1+\text{De}^2)(1+4\text{De}^2)} + \frac{(4-24\text{De}^2)\cos 2\tau + 20\text{De}\sin 2\tau}{(1+\text{De}^2)(1+4\text{De}^2)(1+9\text{De}^2)} \right. \\
&\quad \left. + \frac{(1-35\text{De}^2+24\text{De}^4)\cos 4\tau + (10\text{De}-50\text{De}^3)\sin 4\tau}{(1+\text{De}^2)(1+4\text{De}^2)(1+9\text{De}^2)(1+16\text{De}^2)} \right]
\end{aligned} \tag{42}$$

which has the form of Eq. (16) where:

$$\alpha \equiv \left[\frac{1}{1+\text{De}^2} + \frac{(1-2\text{De}^2)\cos 2\tau + 3\text{De}\sin 2\tau}{(1+\text{De}^2)(1+4\text{De}^2)} \right] \tag{43}$$

and:

$$\beta \equiv \frac{1}{4} \left[\frac{3}{(1+\text{De}^2)(1+4\text{De}^2)} + \frac{(4-24\text{De}^2)\cos 2\tau + 20\text{De}\sin 2\tau}{(1+\text{De}^2)(1+4\text{De}^2)(1+9\text{De}^2)} \right. \\
\left. + \frac{(1-35\text{De}^2+24\text{De}^4)\cos 4\tau + (10\text{De}-50\text{De}^3)\sin 4\tau}{(1+\text{De}^2)(1+4\text{De}^2)(1+9\text{De}^2)(1+16\text{De}^2)} \right] \tag{44}$$

We examine all Padé approximants of Eq. (16) up to order $[4,4]$ and we find exactly two Padé approximants, that we next list in order of degree, first of their numerators, then, denominators. Approximant of order $[1,2]$ of Eq. (16) is given by:

$$\mathbb{N}_1(\tau) = -\frac{\alpha^2 \text{Wi}}{\alpha + \beta \text{Wi}^2} \tag{45}$$

and of order $[1,4]$, by:

$$\mathbb{N}_1(\tau) = \frac{-\alpha^3 \text{Wi}}{\alpha^2 + \alpha\beta \text{Wi}^2 + \beta^2 \text{Wi}^4} \tag{46}$$

Eq. (46) is the second main result of this work. We can also report that this $[1,4]$, approximant the correct limiting behavior for linear viscoelasticity:

$$\lim_{\text{Wi} \rightarrow 0} \mathbb{N}_1(\tau) = \lim_{\text{Wi} \rightarrow 0} \frac{-\alpha^3 \text{Wi}}{\alpha^2 + \alpha\beta \text{Wi}^2 + \beta^2 \text{Wi}^4} = 0 \tag{47}$$

as it should, and that for its behavior in steady shear flow, we get:

$$\lim_{\text{De} \rightarrow 0} \mathbb{N}_1(\tau) = \lim_{\text{De} \rightarrow 0} \frac{-\alpha^3 \text{Wi}}{\alpha^2 + \alpha\beta \text{Wi}^2 + \beta^2 \text{Wi}^4} = \frac{-2 \text{Wi}}{1 + \text{Wi}^2 + \text{Wi}^4} \tag{48}$$

or that:

$$\frac{\Psi_1}{2\eta_0\lambda} = \frac{1}{1 + \text{Wi}^2 + \text{Wi}^4} \quad (49)$$

which is only a close approximation to Eq. (84) of [7]:

$$\frac{\eta}{\eta_0} = \frac{\Psi_1}{2\eta_0\lambda} = \frac{1}{1 + \text{Wi}^2} \quad (50)$$

and so the limiting behavior of Eq. (46), though qualitatively correct, is only approximately right. Since the denominator in Eq. (46) features no real roots, Eq. (46) presents no problematic singularities.

In Section III below, we will compare the Padé approximants, Eq. (45) and (46), with the approximate solution from which this was derived, Eq. (42), and then with the exact solution [Eq. (41) with Eqs. (22)-(27)]. Exploring the Padé table beyond the order $[4, 4]$ may uncover more accurate, though no less complex, approximants. Given the usefulness of our $[1, 4]$ approximant, we chose not to investigate orders exceeding $[4, 4]$.

III. RESULTS

When using the exact solutions given by either Eq. (21) or Eq. (41) with approximate solutions, one must decide on the number of terms to keep in the Bessel functions, and also on how many harmonics to keep in the stress calculations. For the Bessel functions, we find 40 terms to be more than sufficient for our results to be at least invariant to within a line width for all of the figures reported in this paper, and so we kept 40 terms for the Bessel functions throughout. For our figures, we use a computer to evaluate the exact solutions given by Eqs. (21) or (41). For our alternant loop evaluations, we included 40 harmonics, and coded Eqs. (41) and into MATLAB (Version R2012b). On a MacBook Air (1.3 GHz Intel Core i5 processor with 4GB 1600 MHz DDR3 memory) employing the OS X (Version 10.9.5) operating system, we find such an evaluation to consume less than 5 minutes of CPU time. Keeping 40 terms in the Bessel functions, with 40 harmonics in the Fourier series represents an abundance of caution. In all of our figures below, the loops for the exact solution have thus been calculated to a precision that falls well below the line widths.

Figure 2 through Figure 5 illustrate the improvements in the predictions for the shear stress that we realize when we covert Eq. (28) to its $[0, 2]$, $[0, 4]$, $[2, 2]$ and $[2, 4]$ Padé approximants given by Eqs. (32) through (35). In Figure 5, we discover stunning improvement upon Eq. (28) with the $[2, 4]$ approximant, which agrees with the exact solution [Eq. (21) with Eqs. (22)-(25) and with (23)-(27)]. By *stunning*, we mean that although Eq. (28) involves only up to the fifth harmonic (and then only a first approximation of this fifth), the $[2, 4]$ approximant of Eq. (28) agrees closely with the exact solution, which, of course, contains all of the higher harmonics. We learn that with the use of Padé approximants, for the shear stress in large-amplitude oscillatory shear flow, one can take a power series expansion in the shear rate amplitude, truncated after the fourth power of the Weissenberg number (as thus, truncated after the first term

to contain the fifth harmonic), and then get loops that agree closely with the exact solution (even under extreme conditions for the Weissenberg number). Since obtaining the first few terms of a power series in the shear rate amplitude is laborious, even for the simplest relevant constitutive models [7,19,29,30], we recommend the use of Padé approximants to get the most out of this labor.

From Table I we learn that solutions of the form of Eq. (15) are much more commonly available than that of Eq. (14). In this sense, the successful Padé approximation of Eq. (15) would be of wider use. Figure 6 and Figure 7 illustrate the improvements in the predictions for the shear stress that we realize when we convert Eq. (39) [which has the form of Eq. (15)] to its $[0,2]$ and $[0,4]$ Padé approximants given by Eqs. (32) and (40). In Figure 7, we find satisfactory agreement with the exact solution for the shear stress [Eq. (21) with Eqs. (22)-(27)], but the result is not stunning. Specifically, the $[0,4]$ approximant yields a little two-fold asymmetry in the shear stress loops, which makes the prediction slightly unphysical. Otherwise, the agreement with the exact solution is close.

Figure 8 and Figure 9 illustrate the improvements in the predictions for the normal stress differences that we realize when we convert Eq. (42) [which has the form of Eq. (16)] to its $[1,2]$ and $[1,4]$ Padé approximants given by Eqs. (45) and (46). In Figure 9 we find satisfactory agreement with the exact solution for the normal stress differences [Eq. (41) with Eqs. (22)-(27)], but the result is not stunning. Specifically, the $[1,4]$ approximant yields a huge improvement over Eq. (42), shares the same shape as the exact solution, but falls just below the exact solution.

From Figure 7 or Figure 9 of our results, we learn that even for the most highly truncated forms published for analytical solutions, which are always arrived laboriously, it pays to use Padé approximants when using theory or when comparing theory with experimental measurements. Here, specifically, we have examined Eqs. (39) and (42) for the corotational Maxwell model as examples of the truncated forms, Eqs. (15) and (16).

IV. CONCLUSION

This work begins by noticing, from our examination of Table I, that analytical solutions to large-amplitude oscillatory shear flow problems often take the form of truncated expansions in the shear rate [Eqs. (14), (15) and (16)]. Recognizing that getting even the first few terms of such expansion, for even the simplest of relevant constitutive models [7,19,29,30], is laborious. We were thus motivated to devise a method to help make the most of the three common truncations of these expansions (for both the shear stress and the normal stress differences) using Padé approximants.

For the shear stress, when the expansion is truncated after the fourth power of the Weissenberg number, we find stunning accuracy in the $[2,4]$ Padé approximant (see Figure 5). When the expansion is truncated after the second power of the shear rate amplitude (as is more commonly done), we find satisfactory accuracy in the $[0,4]$ Padé approximant (see Figure 7). For the normal stress differences, when the expansion is truncated after the third power

of the Weissenberg number, we find satisfactory accuracy in the $[1,4]$ Padé approximant (see Figure 9).

From this work, we learn that even for the most severely truncated forms published for analytic solutions, it pays to use Padé approximants when evaluating theory or when comparing it with experimental measurements.

V. ACKNOWLEDGMENT

We thank R. Byron Bird, Professor Emeritus of Chemical and Biological Engineering, of the Rheology Research Center of the University of Wisconsin-Madison for his encouragement and helpful discussions.

The financial support of the Royal Golden Jubilee Program of the Thailand Research Fund for (Contract No. PHD/0116/2554) is also greatly appreciated. A.J. Giacomin is indebted to the Faculty of Applied Science and Engineering of Queen's University at Kingston, for its support through a Research Initiation Grant (RIG). This research was undertaken, in part, thanks to funding from the Canada Research Chairs program of the Government of Canada of the Tier 1 Canada Research Chair in Rheology.

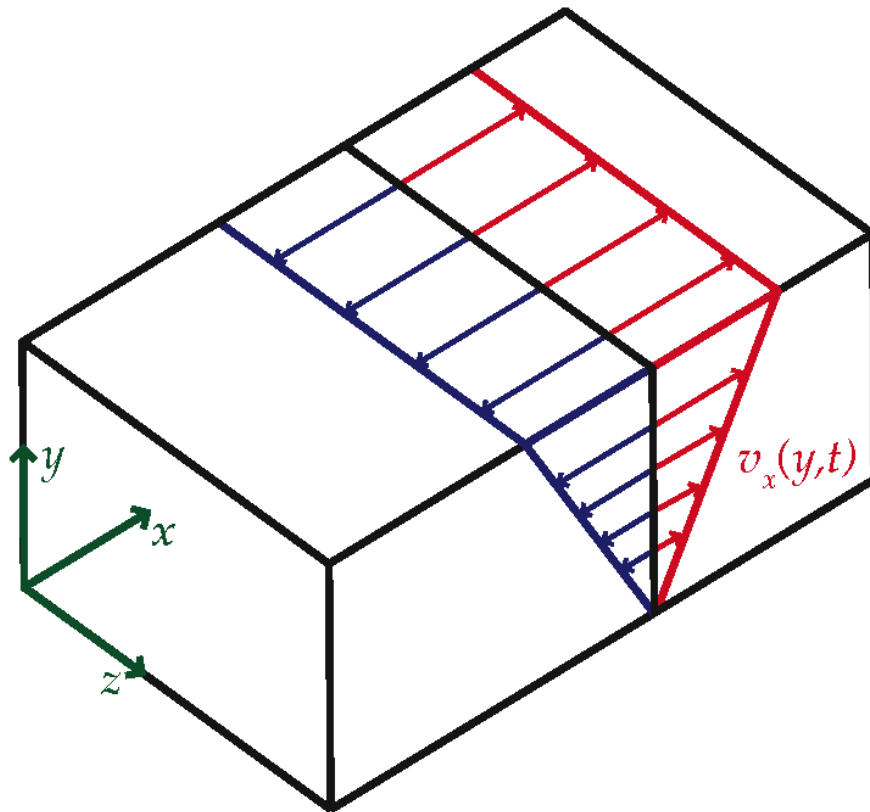


Figure 1: Orthomorphic isometric sketch of alternating velocity profile in oscillatory shear flow [Eq. (1)]. Cartesian coordinates with origin on the stationary plate. The linear velocity profile results from the assumption that inertial effects can be neglected.

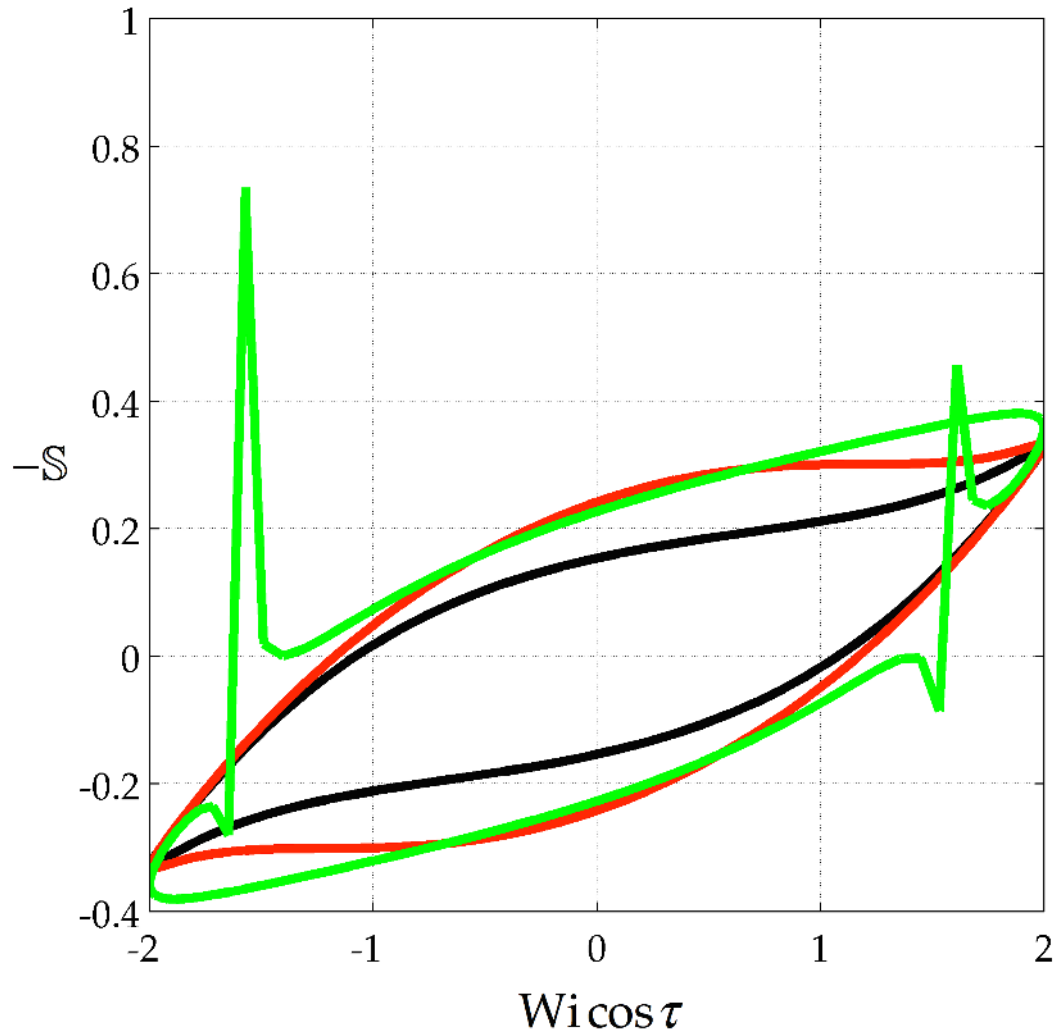


Figure 2. $[0,2]$ Padé approximant of Eq. (28) (**green**) versus Eq. (28) (**red**) and also versus exact solution [Eq. (21) with Eqs. (22)-(27)] (**black**) for alternance. Counterclockwise loops of minus dimensionless shear stress, $-S$, versus dimensionless shear rate, $\lambda\dot{\gamma}$, calculated for the 2-constant corotational Maxwell model with $Wi/De = 2$ and $\lambda\omega = 1$.

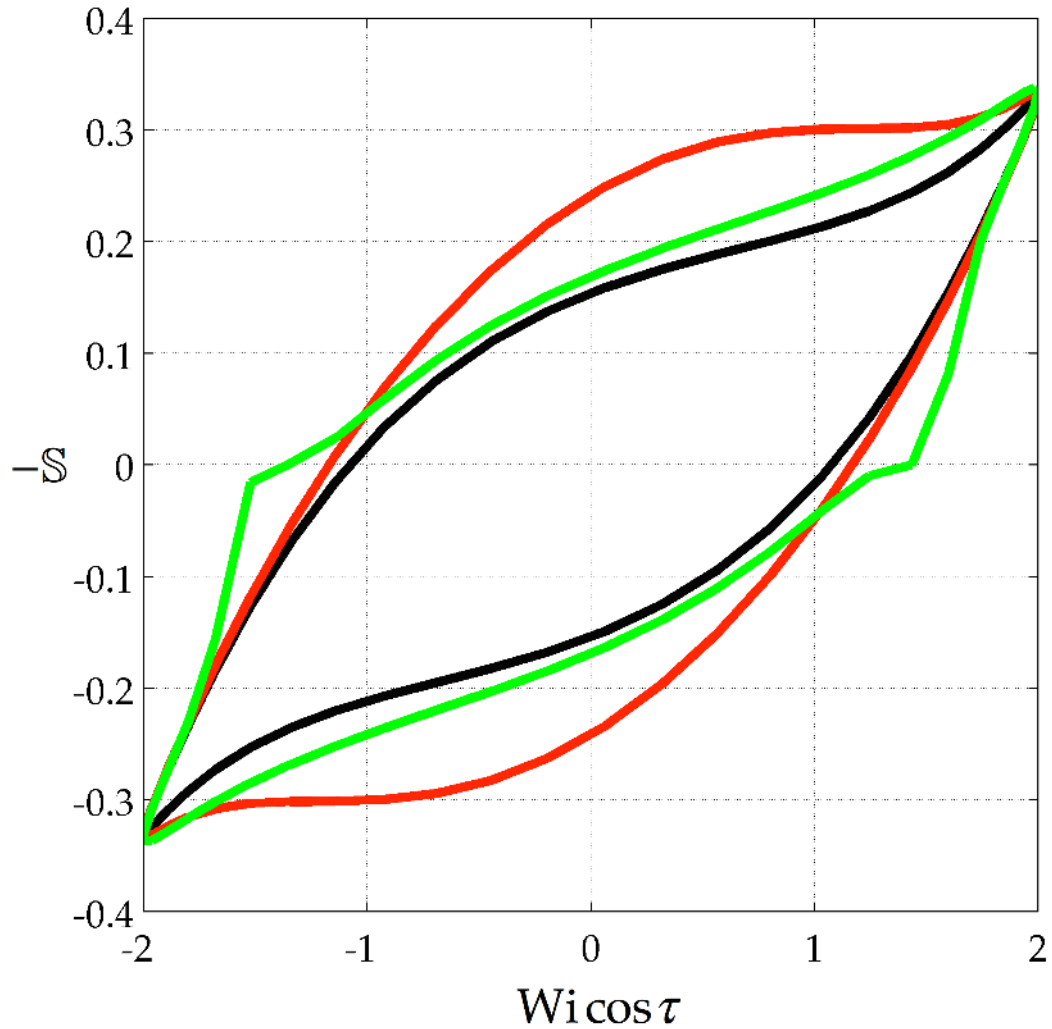


Figure 3. $[0, 4]$ Padé approximant of Eq. (28) (**green**) versus Eq. (28) (**red**) and also versus exact solution [Eq. (21) with Eqs. (22)-(27)] (**black**) for alternance. Counterclockwise loops of minus dimensionless shear stress, $-S$, versus dimensionless shear rate, $\lambda\dot{\gamma}$, calculated for the 2-constant corotational Maxwell model with $Wi/De = 2$ and $\lambda\omega = 1$.

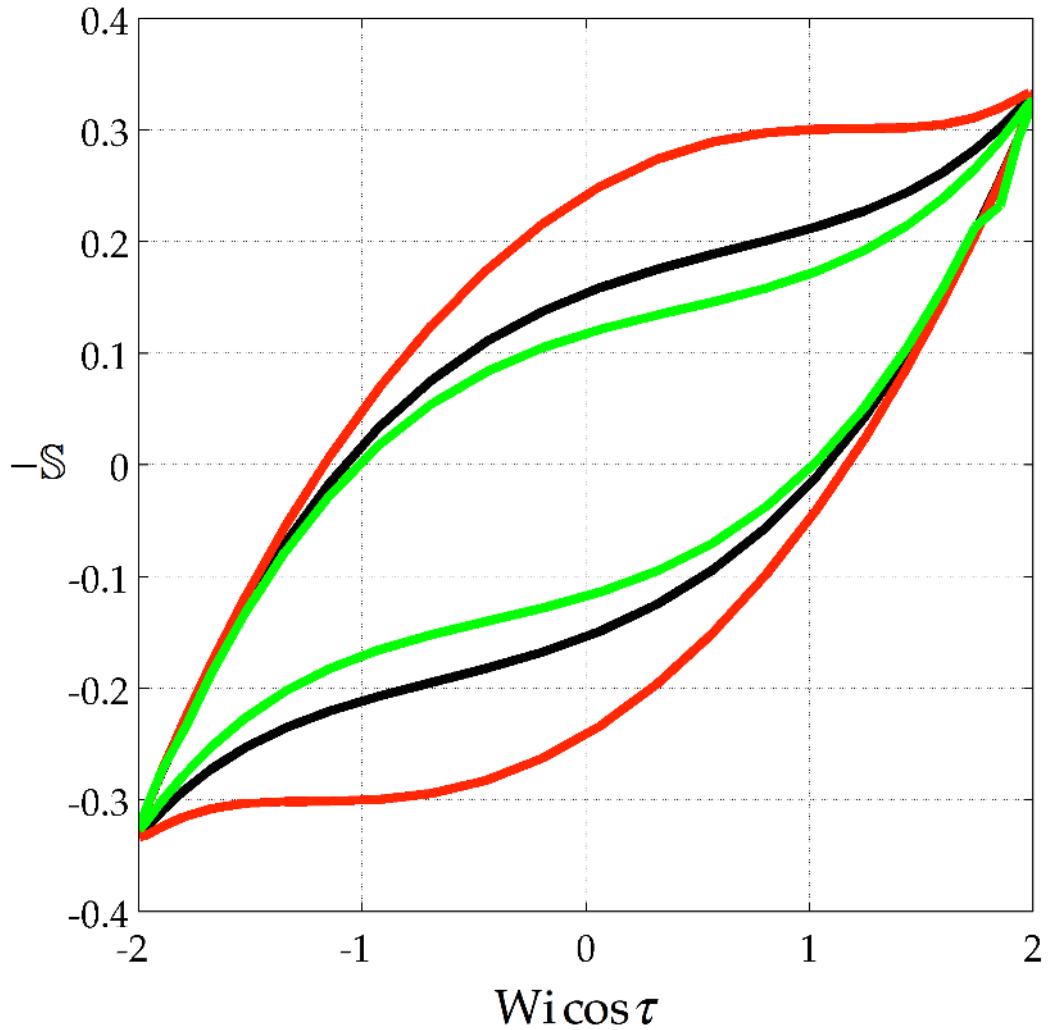


Figure 4. $[2,2]$ Padé approximant of Eq. (28) (**green**) *versus* Eq. (28) (**red**) and also *versus* exact solution [Eq. (21) with Eqs. (22)-(27)] (**black**) for alternance. Counterclockwise loops of minus dimensionless shear stress, $-S$, *versus* dimensionless shear rate, $\lambda\dot{\gamma}$, calculated for the 2-constant corotational Maxwell model with $Wi/De = 2$ and $\lambda\omega = 1$.

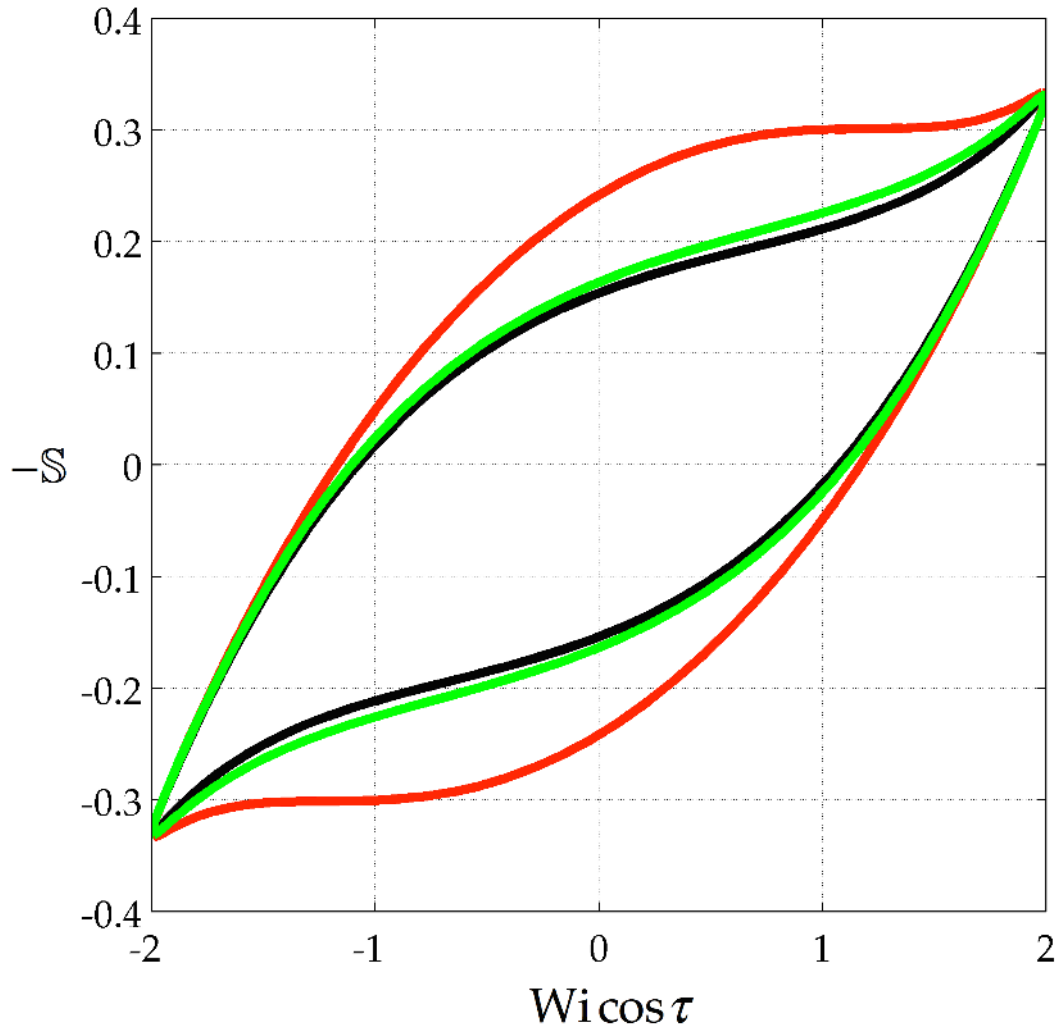


Figure 5. $[2,4]$ Padé approximant of Eq. (28) (**green**) versus Eq. (28) (**red**) and also versus exact solution [Eq. (21) with Eqs. (22)-(27)] (**black**) for alternance. Counterclockwise loops of minus dimensionless shear stress, $-S$, versus dimensionless shear rate, $\lambda\dot{\gamma}$, calculated for the 2-constant corotational Maxwell model with $Wi/De = 2$ and $\lambda\omega = 1$.

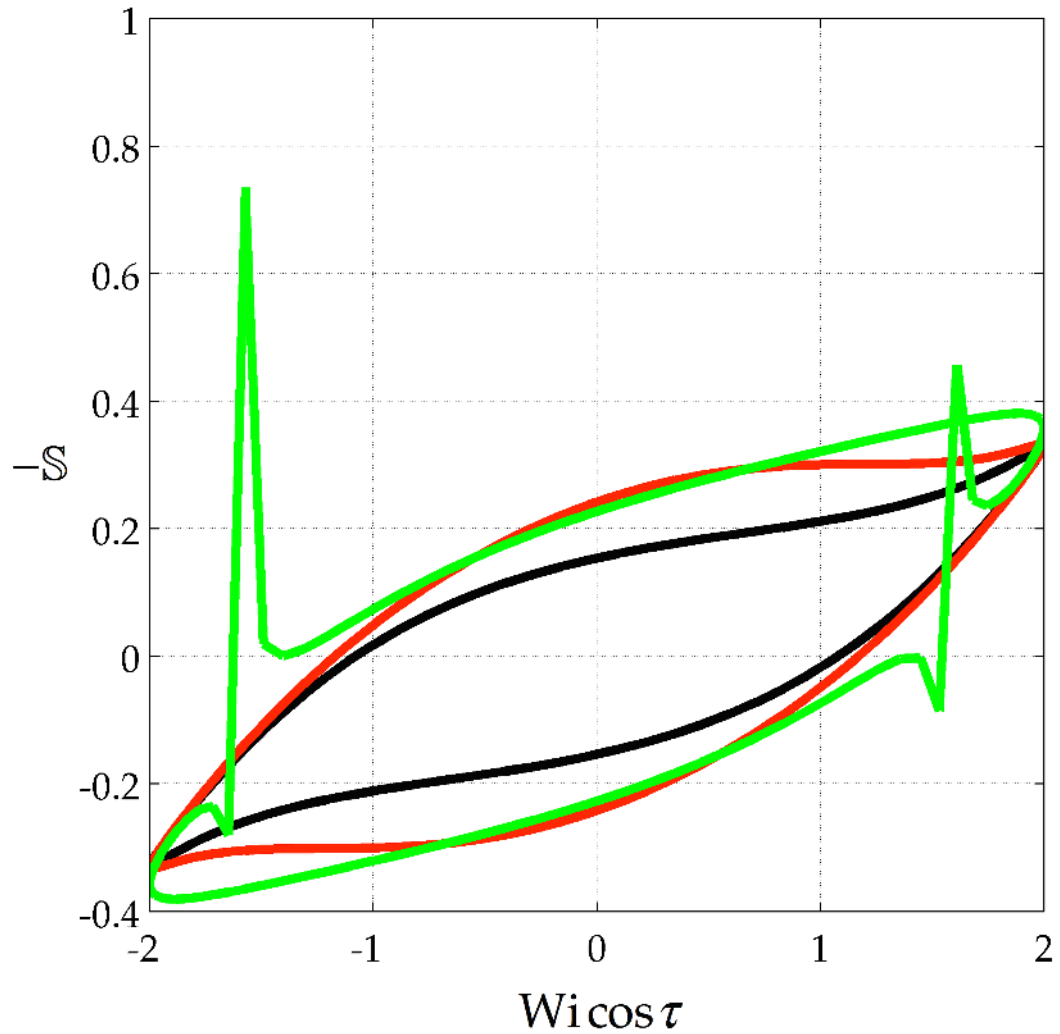


Figure 6. $[0,2]$ Padé approximant of Eq. (39) (**green**) versus Eq. (39) (**red**) and also versus exact solution [Eq. (21) with Eqs. (22)-(27)] (**black**) for alternance. Counterclockwise loops of minus dimensionless shear stress, $-S$, versus dimensionless shear rate, $\lambda\dot{\gamma}$, calculated for the 2-constant corotational Maxwell model with $Wi/De = 2$ and $\lambda\omega = 1$.

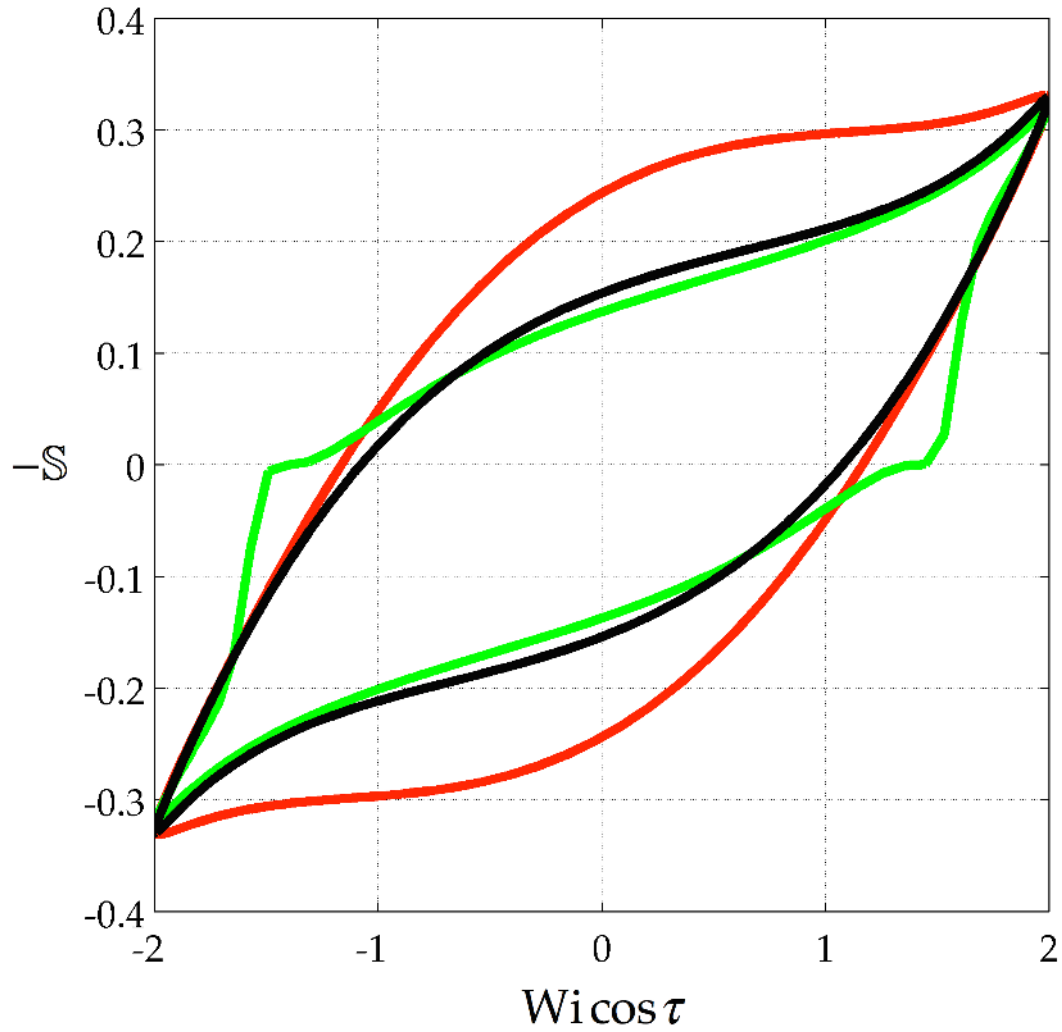


Figure 7. $[0, 4]$ Padé approximant of Eq. (39) (**green**) versus Eq. (39) (**red**) and also versus exact solution [Eq. (21) with Eqs. (22)-(27)] (**black**) for alternance. Counterclockwise loops of minus dimensionless shear stress, $-S$, versus dimensionless shear rate, $\lambda\dot{\gamma}$, calculated for the 2-constant corotational Maxwell model with $Wi/De = 2$ and $\lambda\omega = 1$.

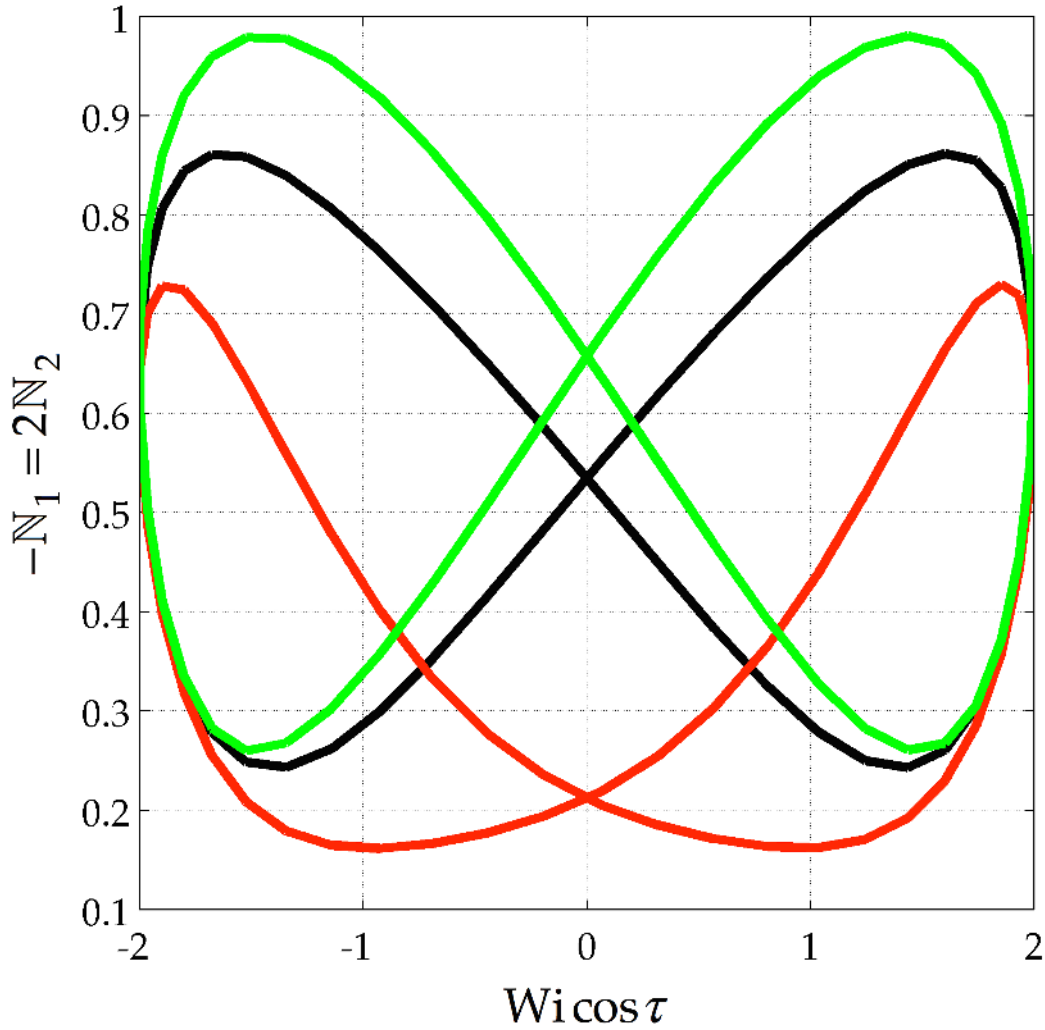


Figure 8. $[1, 2]$ Padé approximant of Eq. (42) (**green**) versus Eq. (42) (**red**) and also versus exact solution [Eq. (41) with Eqs. (22)-(27)] (**black**) for alternance versus $[x, y]$. Minus dimensionless first normal stress differences, $-\mathbb{N}_1 = 2\mathbb{N}_2$, versus dimensionless shear rate, $\lambda\dot{\gamma}$, left-clockwise loops calculated for the 2-constant corotational Maxwell model with $Wi/De = 2$ and $\lambda\omega = 1$.

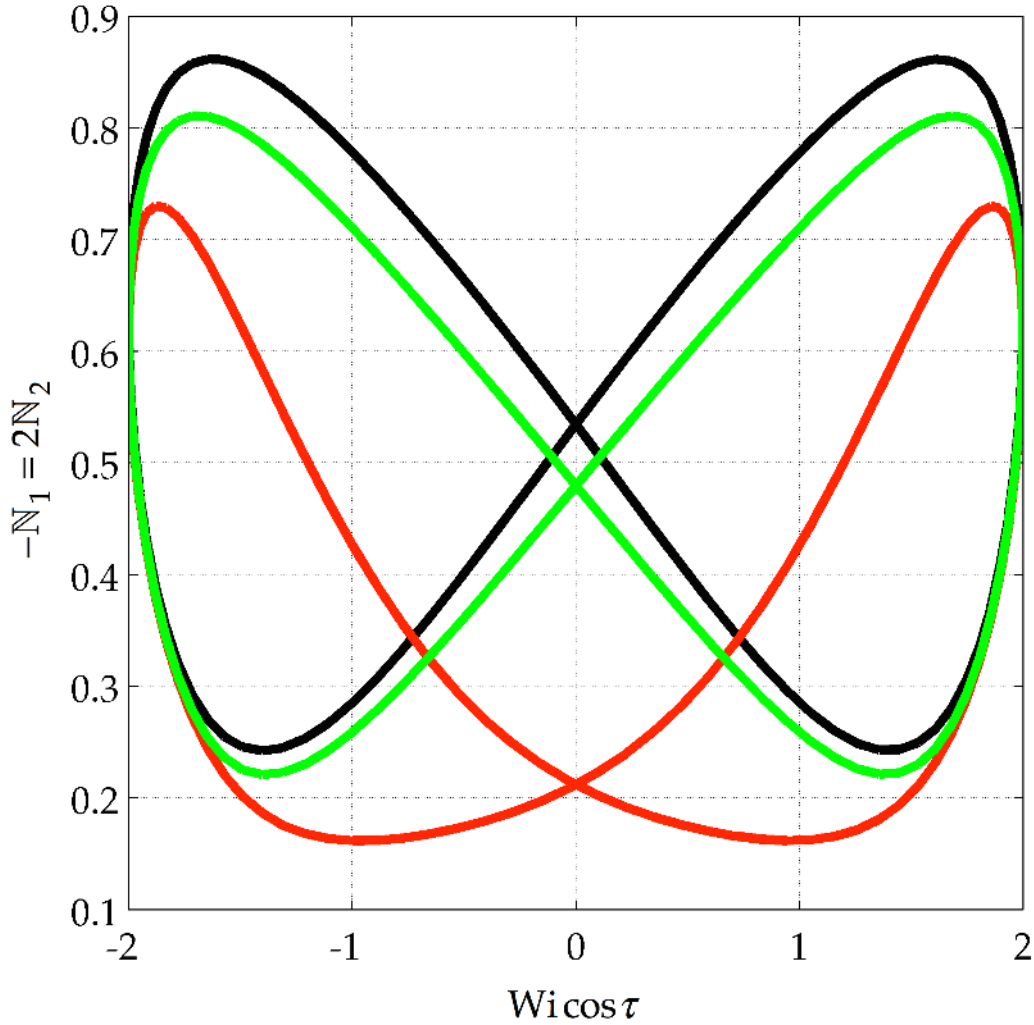


Figure 9. $[1,4]$ Padé approximant of Eq. (42) (**green**) versus Eq. (42) (**red**) and also versus exact solution [Eq. (41) with Eqs. (22)-(27)] (**black**) for alternance versus $[x, y]$. Minus dimensionless first normal stress differences, $-\mathbb{N}_1 = 2\mathbb{N}_2$, versus dimensionless shear rate, $\lambda\dot{\gamma}$, left-clockwise loops calculated for the 2-constant corotational Maxwell model with $Wi/De = 2$ and $\lambda\omega = 1$.

Table I: Literature on Analytical Solutions for Large-Amplitude Oscillatory Shear Flow

	Model	First	Third	Fifth	Zeroth	Second	Fourth	Startup	Notation Eq. $\begin{pmatrix} \tau_{yx} \\ N_1 \end{pmatrix}$	Form	[Ref.] (Correction to)
		Shear Stress Harmonic			Normal Stress Difference Harmonic						
Kirkwood and Plock (1956, 1967); Plock (1957)	RD^h, SK^h	n							(12)	\cong	[31,32,33]
Lodge (1961, 1964)	L^\dagger	ℓ			N_1	N_1				$=$	[34,35]
Spriggs (1966)	NGJ	ℓ			N_1	N_1				$=$	[36]
Spriggs (1966)	CJ	ℓ			N_1 N_2	N_1 N_2				$=$	[36]
Williams and Bird (1962)	O_3	ℓ				N_1				$=$	[37]
Williams and Bird (1964)	O_3	ℓ			N_1	N_1				$=$	[38]
Spriggs (1965)	O_3^\dagger	ℓ			N_1 N_2	N_1 N_2				$=$	[39]
Akers and Williams (1969)	RZ				N_1	N_1				$=$	[40]
Paul (1969); Paul (1970); Bharadwaj (2012)	RD^h, SK^h	n	X						(12)	\cong	[41,42,43] (31,33)
Walters and Jones (1970); Walters (1975)	I_3	n	X							\cong	[44]; Section 6.2.3 of [45]
Paul and Mazo (1969), Paul (1970)	RR^h	n	X						(12)	\cong	[46,42]
MacDonald, Marsh and Ashare (1969)	BC, OWFS [†]	n								\cong	[47]
Bird, Warner and Evans (1971)	RD	n			N_1 N_2	N_1 N_2			(12)	\cong	[48]
Leal and Hinch (1972)	RSD	ℓ			N_1 N_2	N_1 N_2			$\begin{pmatrix} 12 \\ 13 \end{pmatrix}$	\cong	Section 3.3 of [49]
Abdel-Khalik <i>et al.</i> (1974); Bird <i>et al.</i> (1974)	GE+SK	n			N_1 N_2	N_1 N_2				\cong	[50,51]

Bird <i>et al.</i> (1977)	BHS	ℓ	0	0						=	Table 11.4-2 [52]
Mou and Mazo (1977)	RR ^h				N_1 N_2	N_1 N_2				\cong	[53](46)
Pearson and Rochefort (1982); Helfand and Rochefort (1982)	R [†]	n	X						(11)	\cong	[15,16]
Fan and Bird (1984)	CB [†]	n	X						(12)	\cong	[18](16)
Oakley (1992); Oakley and Giacomini (1994)	L [†]	ℓ			N_1	N_1				=	APPENDIX B of [54]; [55](34)
Phan-Thien <i>et al.</i> (2000)	Dough	ℓ								=	[56]
Yu <i>et al.</i> (2002); Zhou (2004)	SE	n	X		N_1	N_1	N_1			\cong	[57,58]
Cho <i>et al.</i> (2010)	K-BKZ								(11)		[59]
Hoyle (2010)	PP	n							(11)	\cong	[60]
Wagner <i>et al.</i> (2011)	R	n	X						(11)	\cong	[61]
Gurnon and Wagner (2012)	G	ℓ	X		N_1 N_2	N_1 N_2			(11)	\cong	[62]
Giacomini <i>et al.</i> (2011)	CM [†] , CJ	n	X	X	N_1 N_2	N_1 N_2	N_1 N_2	X	(12) (13)	\cong	[7](63)
Giacomini and Bird (2011)	ANSR	n	X	X	N_1 N_2	N_1 N_2	N_1 N_2	X	(12) (13)	\cong	[64]
Bird <i>et al.</i> (2014)	RD	n	X						(12)	\cong	[19]
Schmalzer <i>et al.</i> (2014)	RD				N_1 N_2	N_1 N_2	N_1 N_2		(13)	\cong	[29,30,65]
Saengow <i>et al.</i> (2014)	CM	n	X	X	N_1 N_2	N_1 N_2	N_1 N_2	X	(21) (41)	=	[66]
Thompson and de Souza Mendes (2015)	MSJ	n			0	0	0	0		\cong	See Section 5.2.2 of [67]
Bozorgi (2014); Bozorgi and Underhill (2014)	AS ^h	n	X						(11)	\cong	Chapter 8 of [68]; [69]
This paper	CM	n	X	X	N_1 N_2	N_1 N_2	N_1 N_2		(35) (46)	\cong	

Legend: ANSR \equiv corotational; ANSR; AS \equiv active rod suspensions; BC \equiv Bird-Carreau; BHS \equiv Bead-Hookean spring; CB \equiv Curtiss-Bird; CJ \equiv corotational Jeffreys; CM \equiv corotational Maxwell; GE \equiv Goddard integral expansion; L \equiv Lodge rubberlike; NGJ \equiv nonlinear Generalized Jeffreys; O₃ \equiv 3-constant Oldroyd; OWFS \equiv modified Oldroyd-Walters-Fredrickson-Spriggs; PP \equiv pompom; R \equiv reptation; RD \equiv rigid dumbbell; RR \equiv planar rigid ring; RZ \equiv Rouse-Zimm; SE \equiv simple

emulsion; SK = shish-kebab; N_1, N_2 = first and second normal stress differences; $n \equiv \eta^*(\omega, \gamma_0)$; $\ell \equiv \eta^*(\omega)$; † = multiple relaxation times; = = exact; \cong = approximate; ^h = with hydrodynamic interaction.

Table II: Dimensional Variables

Angular frequency	t^{-1}	ω
Cartesian coordinate	L	x, y, z
Elastic Fourier modulus	M/Lt^2	G'_n
Extra stress tensor*	M/Lt^2	$\mathbf{\tau}$
Extra stress, ij th component	M/Lt^2	τ_{ij}
First normal stress coefficient	ML^{-1}	Ψ_1
First normal stress difference	M/Lt^2	$N_1 \equiv \tau_{11} - \tau_{22}$
First normal stress Fourier coefficient, in phase with $\cos m\tau$, Eq. (13)	$\frac{\Psi_1}{\dot{\gamma}^{0^{n-1}}}$	$\Psi'_{1,m,n}$
First normal stress Fourier coefficient, out of phase with $\cos m\tau$, Eq. (13)	$\frac{\Psi_1}{\dot{\gamma}^{0^{n-1}}}$	$\Psi''_{1,m,n}$
Fourier coefficients, in phase with $\cos n\tau$, m nth component, Eq. (11)	M/Lt^2	G''_{mn}
Fourier coefficients, out of phase with $\cos n\tau$, m nth component, Eq. (11)	M/Lt^2	G'_{mn}
Loss moduli, in phase with $\cos n\tau$, m nth component, Eq. (12) [70]	M/Lt^2	η'_{mn}
Relaxation time	t	λ
Second normal stress coefficient	ML^{-1}	Ψ_2
Second normal stress difference	M/Lt^2	$N_2 \equiv \tau_{22} - \tau_{33}$
Shear rate, amplitude	t^{-1}	$\dot{\gamma}^0$
Steady shear viscosity	M/Lt	η
Storage moduli, out of phase with $\cos n\tau$, m nth component, Eq. (12) [70]	M/Lt^2	η''_{mn}
Strain rate tensor	t^{-1}	$\mathbf{\dot{\gamma}}$
Strain rate, ij th component	t^{-1}	$\dot{\gamma}_{ij}$
Time	t	t
Velocity vector	L/t	\mathbf{v}
Velocity, i th-components	L/t	v_i
Viscous Fourier modulus	M/Lt^2	G''_n
Vorticity tensor	t^{-1}	$\mathbf{\omega}$
Zero shear rate viscosity	M/Lt	η_0

Legend: M mass; L length; t time

* Where τ_{ij} is the force exerted in the j th direction on a unit area of fluid surface of constant x_i by fluid in the region lesser x_i on fluid in the region greater x_i [71].

Table III: Dimensionless Variables and Groups

Bessel function of first kind, m th order	$J_m(z) \equiv \sum_{k=0}^{\infty} \frac{(-1)^k}{(m+k)!k!} \left(\frac{z}{2}\right)^{m+2k}$
Bessel function of first kind, m th order with argument Wi/De	$J_m \equiv J_m(Wi/De)$
Coefficient, Eq. (24)	$\alpha_k^{(1)}$
Coefficient, Eq. (26)	$\alpha_k^{(2)}$
Coefficient, Eq. (25)	$\beta_k^{(1)}$
Coefficient, Eq. (27)	$\beta_k^{(2)}$
Deborah number	$De \equiv \lambda\omega$
First normal stress difference	$N_1 \equiv N_1/\eta_0\dot{\gamma}^0$
Generalized non-Newtonianness	Gn
Inclination of non-Newtonianness	ϕ
Integral, Eq. (22)	I_1
Integral, Eq. (23)	I_2
Normal stress difference expansion coefficients, Eq. (16)	α, β
Second normal stress difference	$N_2 \equiv N_2/\eta_0\dot{\gamma}^0$
Shear strain amplitude	γ_0
Shear stress	$S \equiv \tau_{21}/\eta_0\dot{\gamma}^0$
Shear stress expansion coefficients, Eq. (14)	A, B, C
Time	$\tau \equiv \omega t = De(t/\lambda)$
Weissenberg number	$Wi \equiv \lambda\dot{\gamma}^0$

VI. REFERENCES

¹ M.H. Padé, "Sur la Représentation Approchée d'une Fonction par des Fractions Rationnelles, *Annales scientifiques de l'É.N.S. 3e série*, tome 9 (1892), p. 3-93 (supplément).

² Baker Jr., G.A., *Essentials of Pade approximants*, Academic Press, New York (1975).

³ A. Cohen, "A Padé approximant to the inverse Langevin function," *Rheologica Acta*, **30**, 270-273 (1991); Erratum: In Eq. (4), $\frac{9}{5}\lambda$ should be $\frac{9}{5}\lambda^3$.

⁴ A. Gemant, "Komplexe Viskosität.," *Naturwissenschaften*, **25**, 406-407 (1935).

⁵ A. Gemant, "The conception of a complex viscosity and its application to dielectrics," *Transactions of the Faraday Society*, No. 175, **XXXI**, Part II, 1582-1590 (November, 1935b); Erratum: The footnote on p. 1583, "¹⁵A. Gemant, *Naturwiss*, 1935, **23**, 406." should be "¹⁵A. Gemant, *Naturwiss.*, 1935, **25**, 406."

⁶ R.B. Bird and A.J. Giacomin, "Who Conceived the Complex Viscosity?," *Rheologica Acta*, **51**(6), 481-486 (2012).

⁷ A.J. Giacomin, R.B. Bird, L.M. Johnson and A.W. Mix, "Large-Amplitude Oscillatory Shear Flow from the Corotational Maxwell Model," *Journal of Non-Newtonian Fluid Mechanics*, **166**(19-20), 1081-1099 (2011). Errata: after Eq. (20), Ref. [10] should be [13]; in Eq. (66), " $20De^2$ " and " $10De^2 - 50De^4$ " should be " $20De$ " and " $(10 - 50De^2)De$ " and so Fig. 15 through Fig. 17 of [30] below replace Figs. 5-7; on the ordinates of Figs. 5-7, $\frac{1}{2}$ should be 2; after Eq. (119), " $(\zeta\alpha)$ " should be " $\zeta(\alpha)$ "; in Eq. (147), " $n - 1$ " should be " $n = 1$ "; in Eqs. (76) and (77), Ψ' and Ψ'' should be Ψ_1' and Ψ_1'' ; throughout, Ψ_1^d , Ψ_1' and Ψ_1'' should be Ψ_1^d , Ψ_1' and Ψ_1'' ; in Eqs. (181) and (182), "1,21" should be "1,2"; in after Eq. (184) and in Eq. (185), " mp " should be " $1,mp$ "; Eq. (65) should be $We/De > \sqrt[h_N]{(h_N + 1)!}$; see also [63] below.

⁸ A.J. Giacomin, "A Sliding Plate Melt Rheometer Incorporating a Shear Stress Transducer," PhD Thesis, Dept. Chemical Engineering, McGill University, Montreal, Canada (1987).

⁹ A.J. Giacomin, T. Samurkas, and J.M. Dealy, "A Novel Sliding Plate Rheometer for Molten Plastics," *Polymer Engineering and Science*, **29**(8), 499-504 (April, 1989).

- ¹⁰ C. Kolitawong, A.J. Giacomin and L.M. Johnson, "Shear Stress Transduction," Cover Article, *Review of Scientific Instruments*, **81**(2), 021301, 1-20 (2010).
- ¹¹ Giacomin, A.J. and Dealy, J.M. "A New Rheometer for Molten Plastics," S.P.E. Tech. Papers, **XXXII**, Proc. 44th Annual Tech. Conf., Society of Plastics Engineers, Boston, MA (May, 1986), pp. 711-714.
- ¹² A.J. Giacomin and J.M. Dealy, "Large-amplitude oscillatory shear," Chapter 4, Collyer, A.A., ed., *Techniques in Rheological Measurement*, Chapman and Hall, London & New York, pp. 99-121 (1993); Kluwer Academic Publishers, Dordrecht, pp. 99-121 (1993).
- ¹³ A.J. Giacomin and J.M. Dealy, "Using large-amplitude oscillatory shear," Chapter 11, Collyer, A.A. and D.W. Clegg, eds., *Rheological Measurement*, 2nd ed., Kluwer Academic Publishers, Dordrecht, Netherlands, pp. 327-356 (1998).
- ¹⁴ K. Hyun, M. Wilhelm, C.O. Klein, K.S. Cho, J.G. Nam, K.H. Ahn, S.J. Lee, R.H. Ewoldt, G.H. McKinley, "A review of nonlinear oscillatory shear tests: analysis and application of large amplitude oscillatory shear (LAOS)," *Prog. Polym. Sci.* **36**, 1697-1753 (2011).
- ¹⁵ D.S. Pearson and W.E. Rochefort, "Behavior of concentrated polystyrene solutions in large-amplitude oscillating shear fields," *J. Polym. Sci.: Pol. Phys. Ed.*, **20**, 83-98 (1982); Errata: on p. 95, e^{ios} should be e^{-ios} in Eq. (A2); after Eq. (A.10), α should be $\sqrt{\omega \tau_d/2}$; and in Eq. (A.11), $\cos x$ should be $\cosh x$.
- ¹⁶ E. Helfand and D.S. Pearson, "Calculation of the nonlinear stress of polymers in oscillatory shear fields," *J. Polym. Sci.: Pol. Phys. Ed.*, **20**, 1249-1258 (1982).
- ¹⁷ W.M. Davis and C.W. Macosko, "Nonlinear dynamic mechanical moduli for polycarbonate and PMMA," *J. Rheol.*, **22**, 53-71 (1978).
- ¹⁸ X.-J. Fan and R.B. Bird, "A kinetic theory for polymer melts VI. Calculation of additional material functions," *J. Non-Newt. Fluid Mech.*, **15**, 341-373 (1984).
- ¹⁹ R.B. Bird, A.J. Giacomin, A.M. Schmalzer and C. Aumnate, "Dilute Rigid Dumbbell Suspensions in Large-Amplitude Oscillatory Shear Flow: Shear Stress Response," *The Journal of Chemical Physics*, **140**, 074904 (2014); Errata: In Eq. (91), η' should be η'' ; In caption to Fig. 3, " $\psi_1[P_2^2 s_2]$ " should be " $\cos 3\omega t$ " and " $\psi_2[P_2^0 c_0, P_2^2 c_2, \dots]$ " should be " $\sin 3\omega t$ ".

²⁰ R.B. Bird, R.C. Armstrong and O. Hassager, *Dynamics of Polymeric Liquids*, Vol. 1, First Edition, Wiley, New York (1977).

²¹ J.G. Oldroyd, "Non-Newtonian effects in steady motion of some idealized elastico-viscous liquids," *Proc. Roy. Soc.*, **A245**, 278-297 (1958).

²² 吴其晔 and 巫静安, "高分子材料流变学 *Polymer Rheology*," 高等教育出版社, 北京市 (2002).

²³ R.G. Larson, *Constitutive Equations for Polymer Melts and Solutions*, Butterworths, Boston (1988).

²⁴ C.D. Han, *Rheology and Processing of Polymeric Materials: Volume I Polymer Rheology*, Oxford University Press, New York (2007).

²⁵ G. Böhme, *Strömungsmechanik nicht-newtonscher Fluide*, B.G. Teubner, Stuttgart (1981).

²⁶ S.I. Abdel-Khalik, O. Hassager and R.B. Bird, "The Goddard expansion and the kinetic theory for solutions of rodlike macromolecules," *J. Chem. Phys.*, **61**, 4312-4316 (1974).

²⁷ R.B. Bird, O. Hassager and S.I. Abdel-Khalik, "Co-rotational rheological models and the Goddard expansion," *AIChE J.*, **20**, 1041-1066 (1974).

²⁸ Bird, R.B., "A Modification of the Oldroyd Model for Rigid Dumbbell Suspensions with Brownian Motion," *Journal of Applied Mathematics and Physics (ZAMP)*, **23**, 157-159 (1972).

²⁹ Schmalzer, A.M., R.B. Bird and A.J. Giacomin, "Normal Stress Differences In Large-Amplitude Oscillatory Shear Flow For Dilute Rigid Dumbbell Suspensions," PRG Report No. 002, QU-CHEE-PRG-TR--2014-2, Polymers Research Group, Chemical Engineering Dept., Queen's University, Kingston, CANADA (April, 2014).

³⁰ Schmalzer, A.M., R.B. Bird and A.J. Giacomin, "Normal Stress Differences in Large-Amplitude Oscillatory Shear Flow for Dilute Rigid Dumbbell Suspensions," *Journal of Non-Newtonian Fluid Mechanics*, <http://dx.doi.org/10.1016/j.jnnfm>. 2014.09.001 (2014); Erratum: Above Eqs. (14) and (25), "significant figures" should be "16 significant figures".

³¹ J.G. Kirkwood and R.J. Plock, "Non-Newtonian viscoelastic properties of rod-like macromolecules in solution," *J. Chem. Phys.*, **24**, 665-669 (1956).

³² P.L. Auer, (Ed.), *Macromolecules (John Gamble Kirkwood Collected Works)*, J. G. Kirkwood and R. J. Plock, "Non-Newtonian viscoelastic properties of rod-like macromolecules in solution," Gordon and Breach, New York, (1967). Errata: On the left side of Eq. (1) on p. 113, ϵ should be $\dot{\epsilon}$. See also Eq. (1) of [31]; In Eq. (2a), G' should be G'' , and in Eq. (2b), G'' should be G' . See Eqs. (117a) and (117b) of [42].

³³ R.J. Plock, "I. Non-Newtonian Viscoelastic Properties of Rod-Like Macromolecules in Solution. II. The Debye-Hückel, Fermi-Thomas Theory of Plasmas and Liquid Metals," PhD Thesis, Yale University, New Haven, CT (June, 1957). Errata: In Eqs. (2.4a), G' should be G'' , and in Eq. (2.4b), G'' should be G' . See Eqs. (117a) and (117b) of [42].

³⁴ A.S. Lodge, *Elastic Liquids*, Academic Press, London (1964). Errata: Eq. (6.40a) should be $s = \alpha \{ \sin \omega t (1 - \cos \omega \tau) + \cos \omega t \sin \omega \tau \}$; Eq. (6.40b) should be $s^2 = \alpha^2 \{ 1 + \cos 2\omega \tau \cos \omega \tau + \sin 2\omega t \sin \omega \tau \} (1 - \cos \omega \tau)$; Eq. (6.41a) should be $p_{11} - p_{22} = \alpha^2 \{ A + B \cos 2\omega t + C \sin 2\omega t \}$; Eq. (6.41b) should be $p_{21} = \alpha \{ D \cos \omega t + A \sin \omega t \}$; in line 4 of p. 113, $\alpha A \cos \omega t$ should be $\alpha D \cos \omega t$; in the sentence preceding Eq. (6.43), and also in Eq. (6.43), "the out-of-phase part of p_{21} " should be "the part of p_{21} that is in-phase with s ".

³⁵ A.S. Lodge, "Recent network theories of the rheological properties of moderately concentrated polymer solutions," in "Phénomènes de Relaxation et de Fluage en Rhéologie Non-linéaire", Editions du C.N.R.S., Paris, (1961), pp. 51-63.

³⁶ T.W. Spriggs, "Constitutive equations for viscoelastic fluids," Ph.D. Thesis, Chemical Engineering Department, University of Wisconsin, Madison, WI (1966).

³⁷ M.C. Williams and R.B. Bird, "Three-constant Oldroyd model for viscoelastic fluids," *Physics of Fluids*, **5**, 1126-1127 (September, 1962).

³⁸ M.C. Williams and R.B. Bird, "Oscillatory behavior of normal stresses in viscoelastic fluids," *Ind. Eng. Chem. Fundam.*, **3**, 42-49 (1964).

³⁹ T.W. Spriggs, "A four-constant model for viscoelastic fluids," *Chemical Engineering Science*, **20**, 931-940 (1965).

⁴⁰ L.C. Akers and M.C. Williams, "Oscillatory Normal Stresses in Dilute Polymer Solutions," *The Journal of Chemical Physics*, **51**(9), 3834-3841 (1969).

- ⁴¹ E. Paul, "Non-Newtonian viscoelastic properties of rodlike molecules in solution: comment on a paper by Kirkwood and Plock," *J. Chem. Phys.*, **51**, 1271-1290 (1969).
- ⁴² E. W. Paul, "Some Non-Equilibrium Problems for Dilute Solutions of Macromolecules; Part I: The Plane Polygonal Polymer," PhD Thesis, Dept. of Chemistry, University of Oregon, Eugene, OR (September, 1970).
- ⁴³ N. A. K. Bharadwaj, "Low Dimensional Intrinsic Material Functions Uniquely Identify Rheological Constitutive Models And Infer Material Microstructure," Masters Thesis, Mechanical Engineering, University of Illinois at Urbana-Champaign, IL (2012).
- ⁴⁴ Walters, K. and T.E.R. Jones, "Further Studies on the Usefulness of the Weissenberg Rheogoniometer," *Proceedings of the Fifth International Congress on Rheology*, Vol. 4, 337-350, University of Tokyo Press, Tokyo; University Park Press, Baltimore (1970).
- ⁴⁵ Walters, K., *Rheometry*, Chapman and Hall, London (1975).
- ⁴⁶ E. W. Paul and R. M. Mazo, "Hydrodynamic Properties of a Plane-Polygonal Polymer, According to Kirkwood-Riseman Theory," *J. Chem. Phys.*, **51**, 1102 (1969).
- ⁴⁷ MacDonald, I.F., B.D. Marsh and E. Ashare, "Rheological behavior for large amplitude oscillatory motion," *Chem. Eng. Sci.*, **24**, 1615-1625 (1969).
- ⁴⁸ R.B. Bird, H.R. Warner, Jr., and D.C. Evans, "Kinetic theory and rheology of dumbbell suspensions with Brownian motion," *Adv. Poly. Sci. (or Fortschr. Hochpolymeren-Forschung.)*, **8**, 1-89 (1971).
- ⁴⁹ L.G. Leal and E.J. Hinch, "The rheology of a suspension of nearly spherical particles subject to Brownian rotations," *J. Fluid Mech.*, **55**(part 4), 745-765 (1972).
- ⁵⁰ S.I. Abdel-Khalik, O. Hassager and R.B. Bird, "The Goddard expansion and the kinetic theory for solutions of rodlike macromolecules," *J. Chem. Phys.*, **61**, 4312-4316 (1974).
- ⁵¹ R.B. Bird, O. Hassager and S.I. Abdel-Khalik, "Co-rotational rheological models and the Goddard expansion," *AIChE J.*, **20**, 1041-1066 (1974).
- ⁵² R. B. Bird, O. Hassager, R. C. Armstrong, and C. F. Curtiss, *Dynamics of polymeric liquids*, vol 2, 1st edn., John Wiley & Sons, Inc., New York (1977).
Erratum: In Problem 11.C.1 d., "and ϕ_2 " should be "through ϕ_4 ".

- ⁵³ C. Y. Mou and R. M. Mazo, "Normal stress in a solution of a plane-polygonal polymer under oscillating shearing flow," *J. Chem. Phys.*, **67**, 5972 (1977).
- ⁵⁴ J.G. Oakley, "Measurement of Normal Thrust and Evaluation of Upper-Convected Maxwell Models in Large Amplitude Oscillatory Shear," Masters Thesis, Texas A&M University, Mechanical Engineering Dept., College Station, TX (March, 1992).
- ⁵⁵ J.G. Oakley and A.J. Giacomin, "A Sliding Plate Normal Thrust Rheometer for Molten Plastics," *Polymer Engineering and Science*, **34**(7), 580-584 (1994).
- ⁵⁶ N. Phan-Thien, M. Newberry and R.I. Tanner, "Non-linear oscillatory flow of a soft solid-like viscoelastic material," *J. Non-Newton. Fluid Mech.*, **92**, 67-80 (2000).
- ⁵⁷ W. Yu, M. Bousmina, M. Grmela and C. Zhou, "Modeling of oscillatory shear flow of emulsions under small and large deformation fields," *J. Rheol.*, **46**, 1401-1418 (2002).
- ⁵⁸ 周持兴, "聚合物加工理论," 科学出版社, 北京市 (2004).
- ⁵⁹ K.S. Cho, K.-W. Song and G.-S. Chang, "Scaling relations in nonlinear viscoelastic behavior of aqueous PEO solutions under large amplitude oscillatory shear flow," *J. Rheol.*, **54**, 27-63 (2010).
- ⁶⁰ D. M. Hoyle, "Constitutive Modelling of Branched Polymer Melts in Non-linear Response," Chapter 4: "Large Amplitude Oscillatory Shear Flow," PhD Thesis, Dept. of Applied Mathematics, University of Leeds, Leeds, England (2010).
- ⁶¹ M. H. Wagner, V. H. Rolón-Garrido, K. Hyun, and M. Wilhelm, "Analysis of medium amplitude oscillatory shear data of entangled linear and model comb polymers," *J. Rheol.*, **55**, 495 (2011).
- ⁶² A. K. Gurnon and N. J. Wagner, "Large amplitude oscillatory shear (LAOS) measurements to obtain constitutive equation model parameters: Giesekus model of banding and nonbanding wormlike micelles," *J. Rheol.*, **56**, 333 (2012).
- ⁶³ Giacomin, A.J., R.B. Bird, L.M. Johnson and A.W. Mix, 'Corrigenda: "Large-Amplitude Oscillatory Shear Flow from the Corotational Maxwell Model," [Journal of Non-Newtonian Fluid Mechanics, **166**, 1081-1099 (2011)],' *Journal of Non-Newtonian Fluid Mechanics*, **187-188**, 48-48 (2012); see also (7) above].
- ⁶⁴ Giacomin, A.J. and R.B. Bird, "Normal Stress Differences in Large-Amplitude Oscillatory Shear Flow for the Corotational "ANSR" Model," *Rheologica Acta*,

50(9), 741-752 (2011); Errata: In Eqs. (47) and (48), “ $20De^2$ ” and “ $10De^2 - 50De^4$ ” should be “ $20De$ ” and “ $10De - 50De^3$ ”.

⁶⁵ Schmalzer, A.M. and A.J. Giacomin, “Orientation in Large-Amplitude Oscillatory Shear,” *Macromolecular Theory and Simulations*, accepted (September 22, 2014).

⁶⁶ Saengow, C., A.J. Giacomin and C. Kolitawong, “Exact Analytical Solution for Large-Amplitude Oscillatory Shear Flow,” PRG Report No. 008, QU-CHEE-PRG-TR--2014-8, Polymers Research Group, Chemical Engineering Dept., Queen’s University, Kingston (November, 2014).

⁶⁷ Thompson, R.L., A.A. Alicke, P.R. de Souza Mendez, “Model-based material functions for SAOS and LAOS analyses,” *Journal of Non-Newtonian Fluid Mechanics*, **215**, 19-30 (2015).

⁶⁸ Bozorgi, Y., “Multiscale Simulation of the Collective Behavior of Rodlike Self-Propelled Particles in Viscoelastic Fluids,” PhD Thesis, Chemical and Biological Engineering, Rensselaer Polytechnic Institute, Troy, NY (2014).

⁶⁹ Bozorgi, Y. and P.T. Underhill, “Large-amplitude oscillatory shear rheology of dilute active suspensions,” *Rheologica Acta*, DOI 10.1007/s00397-014-0806-y (2014).

⁷⁰ Giacomin, A.J. and R.B. Bird, “Erratum: Official Nomenclature of The Society of Rheology: $-\eta$,” *Journal of Rheology*, **55**(4), 921-923 (July / August, 2011).

⁷¹ R.B. Bird, W.E. Stewart and E.N. Lightfoot, *Transport Phenomena*, Revised 2nd ed., Wiley & Sons, New York (2007).